JOURNAL OF GEOPHYSICAL RESEARCH, VOL. 101, NO. D19, PAGES 23,777–23,791, OCTOBER 30, 1996

The long-range transport of southern African aerosols to the tropical South Atlantic

R. Swap,[1] M. Garstang,[1] S.A. Macko,[1] P. D. Tyson,[1,2] W. Maenhaut,[3] P. Artaxo,[4] P. Kållberg,[5,6] and R. Talbot[7]

Abstract. Two episodes of long-range aerosol transport (4000 km) from southern Africa into the central tropical South Atlantic are documented. Stable nitrogen isotope analysis, multi-elemental analysis, and meteorological observations on local and regional scales are used to describe the observed surface aerosol chemistry during these transport episodes. The chemical, kinematic, and thermodynamic analyses suggest that for the central tropical South Atlantic, west Africa between 0° and 10°S is the primary air mass source region (over 50%) during austral spring. Over 70% of all air arriving in the lower and middle troposphere in the central tropical South Atlantic comes from a broad latitudinal band extending from 20°S to 10°N. Air coming from the east subsides and is trapped below the midlevel and trade wind inversion layers. Air from the west originates at higher levels (500 hPa) and contributes less than 30% of the air masses arriving in the central tropical South Atlantic. The source types of aerosols and precursor trace gases extend over a broad range of biomes from desert and savanna to the rain forest. During austral spring, over this broad region, processes include production from vegetation, soils, and biomass burning. The aerosol composition of air masses over and the atmospheric chemistry of the central South Atlantic is a function of the supply of biogenic, biomass burning, and aeolian emissions from tropical Africa. Rainfall is a common controlling factor for all three sources. Rain, in turn, is governed by the large-scale circulations which show pronounced interannual variability. The field measurements were taken in an extremely dry year and reflect the circulation and transport fields typical of these conditions.

1. Introduction

Field measurements of particulate aerosols were made to determine the source characteristics, production, and transport of aerosols over and off southern Africa as part of the Southern African Fire-Atmosphere Research Initiative (SAFARI) [*Andreae et al.*, 1993] and the Transport and Atmospheric Chemistry near the Equator-Atlantic (TRACE-A) [*Fishman et al.*, 1994] experiments carried out in September and October 1992. Among the objectives of these joint research efforts was the investigation of the role of southern hemisphere aerosols in the atmospheric chemistry, climatology, and ecology of the region [*Andreae et al.*, 1993].

Evidence of aerosol production and the subsequent transport into the southern tropical Atlantic off the west coast of southern Africa are examined in this paper. Uncertainties founded in the paucity of long-term meteorological observations to adequately describe the four-dimensional (x,y,z,t) nature of the atmosphere over this region are offset by the simultaneous use of kinematic (trajectory), thermodynamic (vertical structure), and chemical (isotope and elemental tracer) analyses.

Chemical and meteorological analyses are combined to determine the place of origin and the types of aerosols being produced. The place of origin may include the location where precursor gases which lead to the photochemical production of a trace gas such as ozone are produced. Determination of both the origin and the source type under such circumstances allows distinctions to be made between surface and stratospheric sources on regional and continental scales. The observed aerosol, where possible, will be partitioned according to primary biogenic particles, soil dust, biomass burning products, and sea-salt spray components.

2. Background

Aerosol production over southern Africa, particularly between the latitudes of approximately 15°S and 30°S, undergoes a marked seasonality. This seasonality is primarily a function of the pronounced wet and dry seasons which dominate this region [*Tyson*, 1986]. The onset of spring rains over Africa north of about 20°S follows a temporal and spatial progression beginning in June-July for lower latitudes and beginning around October-November for high latitudes. South of about 20°S the progression is from east to west. The production of aerosols from dry soil and vegetation precedes the beginning of the rainy season and is in phase with aerosol and trace gas production from biomass burning. Spring rains over the excessively dry surface also trigger gaseous nitrogen species emissions from the soils and hydrocarbon production from the

[1]Department of Environmental Sciences, University of Virginia, Charlottesville.
[2]On sabbatical from Climatology Research Group, University of the Witwatersrand, Johannesburg, South Africa.
[3]Institute for Nuclear Sciences, University of Gent, Gent, Belgium.
[4]Institute of Physics, University of São Paulo, São Paulo, Brazil.
[5]Swedish Meteorological and Hydrological Institute, Norrköping, Sweden.
[6]Now at European Center for Medium-Range Weather Forecasts, Reading, England.
[7]Institute for the Study of Earth, Oceans and Space, University of New Hampshire, Durham.

Paper number 95JD01049.
0148-0227/96/95JD-01049$09.00

blooming of dormant vegetation [*Williams et al.*, 1992; *Fehsenfeld et al.*, 1992; J.S. Levine, personal communication, 1995]. Synchronous or near-synchronous production in time and space of aerosols and precursor trace gases involved with the formation of O_3 thus occurs from at least three sources. The interdependence of these sources upon rainfall as a common factor means that they are all subject to changes in the regional and larger scale circulation fields which initiate the spring rains.

Aerosols from southern Africa have been observed out over the tropical South Atlantic for over 20 years [*Chester et al.*, 1972; *Parkin et al.*, 1972; *Cachier et al.*, 1986; *Losno et al.*, 1992]. The seasonality of these aerosols has also been noted. *Chester et al.* [1972] found very low aerosol loadings in the South Atlantic during the transition from austral summer to fall. In contrast, *Losno et al.* [1992] observed high concentrations of airborne particulates during the austral winter-spring transition period in a latitudinal belt between the equator and 20°S. These elevated aerosol concentrations were attributed to biomass burning, aeolian erosion, and industry, although no attempt was made to differentiate between these sources. Several authors have measured the elemental composition of biomass burning aerosols in Africa [*Crozat et al.*, 1978; *Crozat*, 1979; *Cachier et al.*, 1985; *Lacaux et al.*, 1993] and South America [*Artaxo et al.*, 1988, 1990]. These aerosols have a distinct elemental profile rich in organic material, potassium, phosphorus, chlorine, zinc, sulfur, and other elements.

Fishman et al. [1991] have noted the summer-fall minimum and winter-spring maximum production of aerosols over southwest Africa and the southern tropical Atlantic. *Annegarn et al.* [1983], *Andreae et al.* [1988], and *Connors et al.* [1991] have all documented contributions from biomass burning, aeolian sources, and industry over the tropical regions of Brazil and southern Africa.

The observation of maximum biomass burning emissions in the southern hemisphere during the austral winter-spring transition coincides with the maximum occurrence of fires on the African continent [*Cahoon et al.*, 1992]. The highest frequency of African biomass burning occurs from 10° to 20°S during the period July to September. Many of the fires in southern Africa are of anthropogenic origin. However, in sparsely populated regions and prior to human population expansions, a significant number of fires are caused by lightning. *Siegfried* [1981], for example, shows that for the Etosha National Park, 70% of the fires are caused by lightning. Lightning accompanies the onset of the spring rains.

Fishman et al. [1990, 1991], using remotely sensed total ozone mapping spectrometer (TOMS) and Stratospheric Aerosol and Gas Experiment (SAGE) data, in which the tropospheric component is derived as a residual from the subtraction of the stratospheric O_3 from total columnar abundance, have suggested that a spring maximum in ozone occurs in the midtroposphere of the tropical South Atlantic. The height of maximum concentrations in ozone at Ascension Island has been shown to lie between 850 and 500 hPa [*Fishman et al.*, 1991]. Attempts have been made to explain the transport meteorology that might initiate and sustain a tropical south Atlantic ozone maximum. *Krishnamurti et al.* [1993], *Fakhruzzaman et al.* [1994], and *Pickering et al.* [1994] have used model-generated large-scale atmospheric circulation fields and trajectory analyses to suggest that an ozone maximum is supported by products derived from biomass burning generated over both southern Africa and Brazil. The possibility of stratospheric intrusions of O_3 contributing to the maximum has also been noted [*Krishnamurti et al.*, 1993].

Previous work has not quantified the sources of the ozone maximum or provided independent substantiating evidence that the sole or even primary source of the precursor gases and aerosol is due to biomass burning. All work to date emphasizes large-scale flow fields in providing an explanation for the Atlantic ozone maximum during austral spring. No attention has been devoted to showing how interannual circulation changes may affect transport patterns or how longer-term, near-decadal changes may also be of importance. That such longer-term changes have occurred over southern Africa is well known [*Tyson*, 1986; *Preston-Whyte and Tyson*, 1988; *Lindesay*, 1988]. The SAFARI was carried out in an extremely dry year, requiring that all interpretations of the findings consider this anomalous condition.

3. Field Measurements and Analytical Methods

Surface particulates were collected at Okaukuejo, Etosha National Park, Namibia (ENP; 16°E, 19°S) and at Ascension Island (AI; 14°W, 8°S). ENP is situated on the interior plateau of southern Africa at an altitude of between 1100 and 1400 m (Figure 1). To the west, the terrain rises gently to the rim of the escarpment, a feature extending from Angola to Malawi in a girdle around the whole subcontinent, before falling to the sea through the dissected country that constitutes the mountains of the escarpment.

Aerosols were collected for stable isotope and for multielemental analyses by particle-induced X ray emission (PIXE) analysis and instrumental neutron activation analysis (INAA). The aerosol sampling was done with vacuum pumps with flow rates of approximately 100 L min^{-1} for the stable isotope

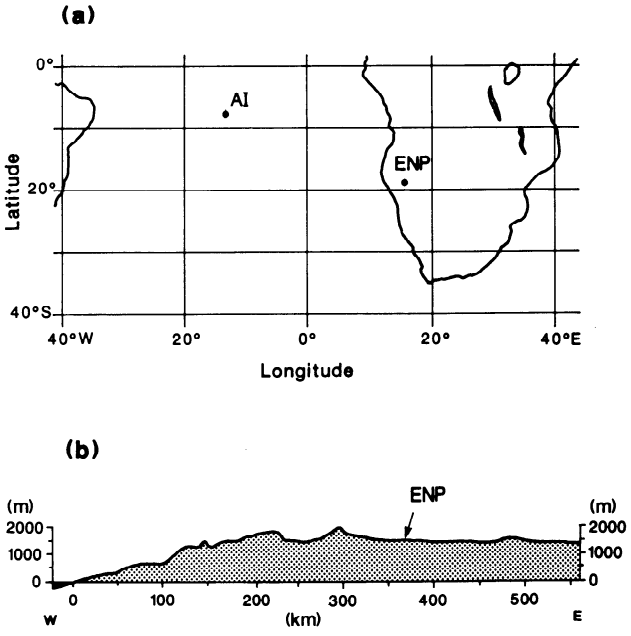

Figure 1. (a) Location of Etosha National Park (16°E, 19°S) and Ascension Island (15°W, 7°S). (b) Topographic relief typical of Namibia, southwestern Africa. The narrow coastal plain, eroded escarpment, and extensive interior plateau are shown. Etosha National Park lies approximately 350 km inland of the coast.

samples and of approximately 20-30 L min^{-1} for the PIXE samples. Glass fiber filters (Gelman type AE) that had been ashed at 500°C were used to collect the aerosols for stable isotope analyses of nitrogen. Particulates for multielemental analysis were sampled using in-line stacked filter units (SFU) containing 47-mm-diameter coarse (8 μm pore size, Apiezon-coated) and fine (0.4 μm pore size) filters [*Cahill et al.*, 1977; *Heidam*, 1981]. Nuclepore polycarbonate filters were used to collect particulates for the multielemental analysis. The SFUs were fitted with specially designed inlets that provided a 50% cutoff for diameters of ≥ 10 μm. The aerosols were separated into two size fractions: coarse, between 2 and 10 μm equivalent aerodynamic diameter (EAD), and fine, > 2 μm EAD [*John et al.*, 1983].

Aerosol samples were taken at a remote savanna site in ENP at a height of 10 m above the surface (~ 1112 m). The nature of the sparse vegetation around the sampling site is a mixture of grasses and shrubs (70%/30%). Aerosol samples were collected on a small hill on the windward side of AI at a height of 2 m above the surface (~ 160 m) due to the physical constraints of the sampler. The nature of the AI surface near the sampling site is exposed soil comprised of volcanic debris the size of small pebbles with almost no vegetation. Aerosol samples for isotope analysis were taken over 12 hour periods beginning at sunrise and sunset (0700 and 1900 South African standard time (SAST). Aerosol samples for multielemental analysis were taken over 24 hours and collected at sunrise. At AI, aerosol-sampling was conducted with a single aerosol sampling device from August 20, 1992, to November 1, 1992, over 48-hour periods. The first fifteen 48-hour periods were dedicated to collecting stable isotope samples and the remaining periods to the collection of multielemental samples.

Aerosol samples collected were subjected to bulk stable nitrogen analysis. Stable nitrogen analysis followed the method of *Macko et al.* [1987]. Aerosol filters were acidified using HCl to remove inorganic carbon. The residue was dried, then sealed along with CuO and Cu in quartz combustion tubes under vacuum. The combustion tubes were then heated to 850°C to convert nitrogenous compounds to gaseous nitrogen. The N_2 gas was then cryogenically separated on a vacuum line and analyzed on a Prism-Isotope Ratio Mass Spectrometer (VG Micromass) for the isotopic signatures.

The SFU filter samples from both ENP and AI were analyzed by PIXE methods that have been described previously [*Maenhaut et al.*, 1981; *Maenhaut and Raemdonck*, 1984; *Johansson and Campbell*, 1988; *Tapper and Malmqvist*, 1991; *Artaxo et al.*, 1993a]. The filters from both sites were also analyzed for total particulate mass using gravimetric techniques. Black carbon content was determined for ENP samples using a light reference technique [*Andreae*, 1983]. Furthermore, the filters from ENP were analyzed by INAA using a procedure similar to that described by *Schutyser et al.* [1978].

3.1. Chemical Results

Two episodes of explicit aerosol transport from the region of ENP to the tropical south Atlantic in the vicinity of AI are presented. The first episode occurred during the AI sampling of aerosols for nitrogen isotope analysis (Figure 2). The second episode was during the sampling at AI for multielemental analyses (Figure 3). Bulk stable nitrogen isotope ratios measured at ENP on September 9 and 10, 1992, are essentially identical to those recorded at AI 6 to 9 days later during the 48-hour periods centered on September 16 and

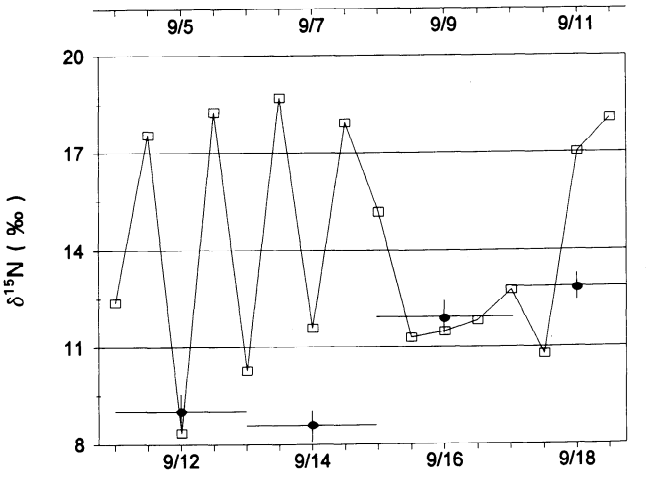

Figure 2. The $\delta^{15}N$ isotope signature time series of surface particulates at ENP (squares) and AI(circles). Upper (ENP) and lower (AI) timescales are offset by 7 days such that the $\delta^{15}N$ signatures coincide. The ENP values are representative of 12-hour sampling periods. The AI values are plotted at the median dates of the 48-hour sampling periods (indicated by horizontal lines). The vertical lines on the AI values are indicative of the range of reproducibility of the bulk stable nitrogen isotope analysis for SAFARI samples (~ 0.5%).

September 18, 1992. Observations of $\delta^{15}N$ at the two stations were distinctly different on the days prior to the episode. The aerosol at AI became increasingly enriched with the onset of the transport episode to reflect the influence of the isotopically heavier terrestrial nitrogen signal [*Sealy et al.*, 1987; *Heaton*, 1987]. The times of earliest detection of the nitrogen portion of the particulate aerosols at ENP and earliest arrival at AI suggest an average transport speed of 7.1 m s^{-1} ranging from 6.6 m s^{-1} to 7.7 m s^{-1} over a distance of 4,000 km between the stations.

The second transport episode uses the results of multielemental analysis of filter samples collected at ENP and AI between September 21 and October 16, 1992. This analysis indicates biomass burning and soil dust signatures in the aerosol fine fraction at AI. Time series of the concentrations of six elements contained in the fine fraction (EAD < 2 μm) filter samples, K, S, Fe, Ca, Al, and Si, are shown in Figure 3. The time series of observations at the two locations have been adjusted for a 7-day time lag between ENP and AI.

The elemental analysis of the aerosols collected at ENP and AI does not show the singular coincidence found in the isotopic analysis. However, the maximum concentrations recorded for at least six elements over the period of September 22 to October 16, 1992, at AI follows a maximum in concentration in that element occurring 5 to 9 days earlier at ENP. Most of the elements (K, Fe, Ca, Al, Si) show higher values at AI 6 to 7 days after increases in that element have been observed at ENP. Sulfur values increase at AI 8 days after a maximum in S is observed at ENP. The elements associated with soil dust, Fe, Al, and Si, show the earliest response at AI after peak concentration values are seen at ENP 5 days earlier. Although all peaks in the concentrations of these six elements at AI can be traced back to higher concentrations at ENP, not all increases in the concentrations observed at ENP are reflected at AI. The range of 5 to 9 days in arrival times of the different chemical species at AI reflects that all species are not produced simulta-

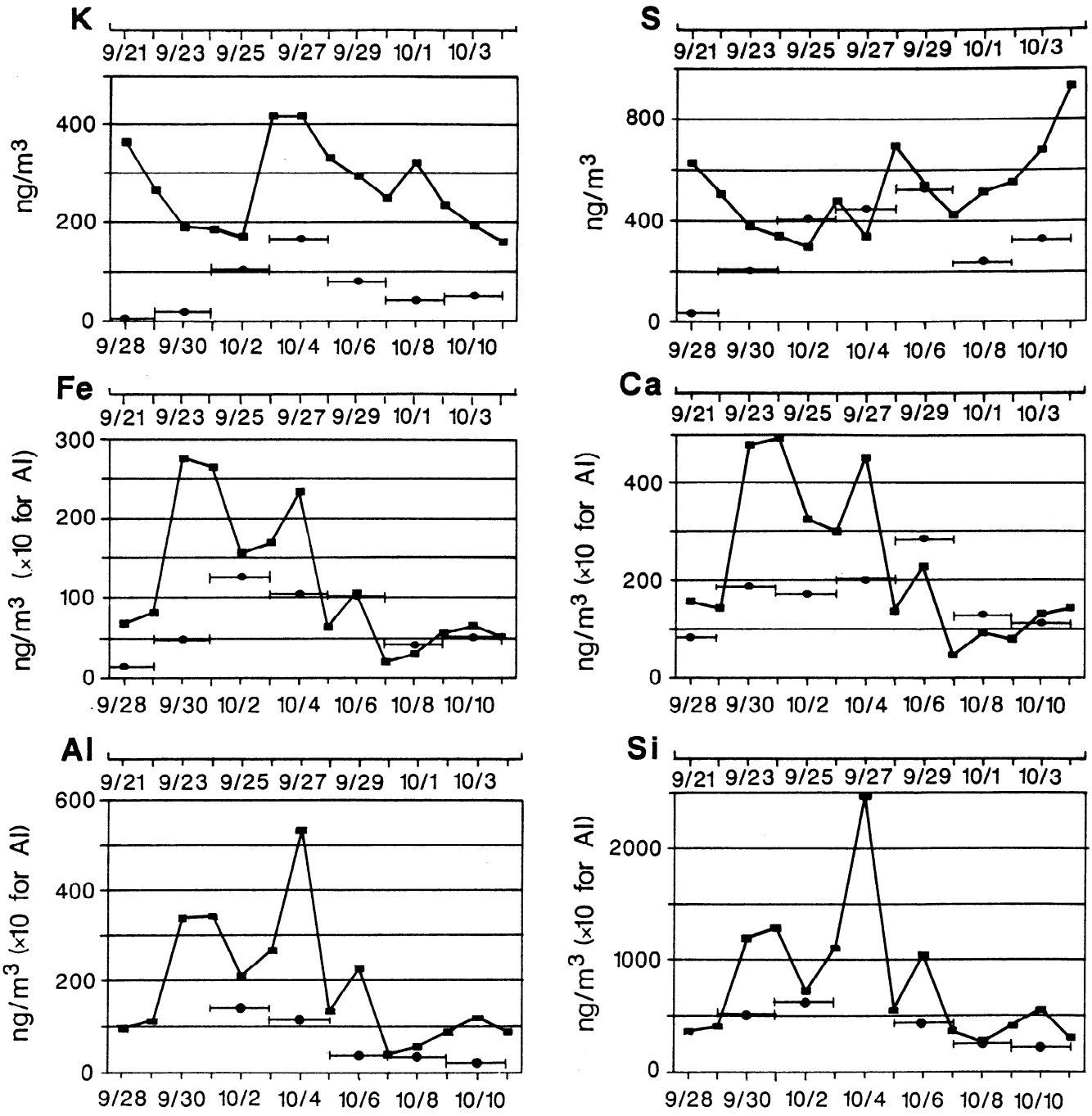

Figure 3. Time series of fine particle fraction (< 2μm EAD) concentrations, in nanograms per cubic meter for ENP (upper timescale) and AI (lower timescale) for K, S, Fe, Ca, Al, and Si. ENP 24-hour average concentrations are indicated with squares. AI 48-hour average concentrations are indicated by the horizontal bars.

neously from any point source. Rather, production varies over a region around the point and over time, which is reflected in the subsequent transport of these species. The episodic production of surface-observed species at ENP and the correlation between this production and wind velocities is dealt with in detail by *Swap* [1995].

Concentrations of soil dust elements decrease during the long-range transport from ENP to AI due to particulate sedimentation. Soil dust sources for these elements are in the region of ENP and reflect higher levels of Fe, Al, Si, and Ca than are normally associated with a well-mixed air mass. An observed decline of over 95% in Fe, Al, Si, and Ca concentrations occurs between ENP and AI for the corresponding peak values at the surface at each station. This is not the case for K and S. Potassium, indicative of both biomass burning and biomass debris, shows a 50% drop in concentration between ENP and AI. This element, if produced by biomass burning and subjected to anticyclonic circulation for several days, would be well-mixed compared to local soil dust inputs. Sulfur shows only a 25% reduction in concentration between ENP and AI at

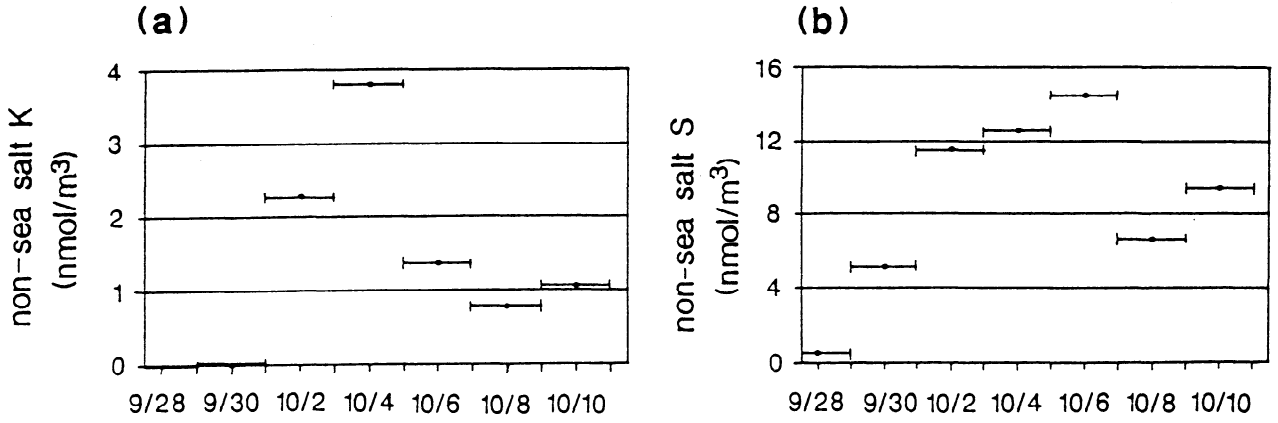

Figure 4. Excess, or non-sea salt, fine fraction (< 2μm) of (a) K aerosol and (b) S aerosol present in surface aerosol samples at AI in nanomoles per cubic meter, where excess K = K(nmol m^{-3}) - [Ca (nmol m^{-3}) * (K/Ca (mol/mol)) in sea water] and excess S = S(nmol m^{-3}) - [Ca (nmol m^{-3}) * (S/Ca (mol/mol)) in sea water].

the times of corresponding peak values. Because S is an element produced not only by biomass burning, but also produced in significant quantities from biogenic marine sources (dimethylsulfide (DMS)) in regions of high productivity such as the Benguellan upwelling, a much smaller drop in S concentration compared to the other five elements can be expected.

Sea salt in the South Atlantic Ocean may also be a major source of particles contributing to the concentrations of elements typical of biomass burning such as K, S, Ca, and P. The ratios between the elements, however, are different between sea-salt aerosol particles and biomass-burning particles transported over long distances [*Artaxo et al.*, 1990]. Figure 4 shows the excess K and S concentrations above values of background marine aerosols. The pronounced excess in non-sea-salt S and K seen from October 1 to October 7, 1992, is coincident with increased soil dust at AI (Figure 3). Thus two signals are evident in Figures 3 and 4: soil dust constituents represented by Fe, Al, and Si and non-sea-salt constituents, K and S, which are ascribed to biomass burning [*Maenhaut et al.*, this issue].

The chemistry for both episodes suggests transport of southern African aerosols from southwestern Africa to the region of AI in the tropical South Atlantic. A representative mean transit time of 6 to 7 days over a straight line distance of 4,000 km is found giving a mean transport speed of 6.6 to 7.7 m s^{-1}. These speeds are consistent with wind speeds in the mixed (~ 500 m) and cloud (500-3,000 m) layers of the south tropical Atlantic [*Riehl*, 1979; *Hastenrath*, 1991].

3.2. Meteorological Results

Daily three-dimensional, 10-day, forward trajectories, starting at ENP, and 10-day, backward trajectories, starting at AI, were calculated using a three-dimensional trajectory package of the Swedish Hydrological and Meteorological Institute [*Kållberg*, 1984; *Garstang et al.*, this issue]. The trajectories are calculated from the six hourly global three-dimensional wind analyses produced by the European Centre for Medium-Range Weather Forecasts (ECMWF). The ECMWF data assimilation scheme is described by *Bengtsson* [1985]. The starting location for the forward trajectories is 16°E, 19°S, in the vicinity of ENP. The backward trajectory starting location is 14°W, 8°S, the approximate location of AI. Five different trajectories, each beginning at a different initial level (900, 850, 800, 700, and 500 hPa), were calculated daily for the entire SAFARI period (August 24-October 18, 1992). Thirteen levels (of the available 31) below 500 hPa are used to calculate air parcel positions every 15 min. Diabatic and adiabatic processes are included in the ECMWF model to calculate vertical velocities. The motion can be forward or backward in time depending upon the sign of the time increment. In the data sparse region of the tropical South Atlantic and Indian Oceans, TOV satellite temperature profiles and Meteosat cloud tracked winds are included as part of the ECMWF data base.

Forward trajectories for September 9, 1992, and the backward trajectories for September 16, 1992, are shown for episode 1 in Figures 5a and 5b. Trajectories that arrive in the AI region as well as all backward trajectories from AI are plotted.

Trajectories originating at ENP on September 9, 1992, at 875, 850, and 800 hPa cross directly over AI 6 to 7 days after leaving ENP (Figure 5a). The 900-hPa backward trajectory originating at AI on September 16, 1992, extends back to the ENP region over a period of 6 to 7 days (Figure 5b). Trajectories at higher levels extend back to the continent over intervals of up to 10 days and to originating locations which extend over a wide latitudinal belt from 20°S to 15°N.

Forward and backward trajectories for episode 2 (Figure 6) show a connection between ENP and AI similar to that shown for episode 1. This low-level transport from ENP to AI is only seen twice for a total of 8 days over the 48-day SAFARI observational period. An in-depth discussion of the air parcel transport statistics is presented later in this section. Direct communication between the two localities occurs in the low levels and is absent at the higher levels. Backward trajectories from AI once again originate over a broad latitudinal band of Africa (0°S to 30°S).

Transport between the surface and the middle and upper troposphere is likely to be inhibited by temporally persistent and spatially ubiquitous stable layers in the tropical latitudes [*Garstang et al.*, this issue]. Daily and near-daily rawinsoundings launched from ENP and AI are used to find absolutely stable layers in a time series for both stations (Figure 7). Absolute stability is defined when the environmental lapse rate is less than the wet adiabatic lapse rate.

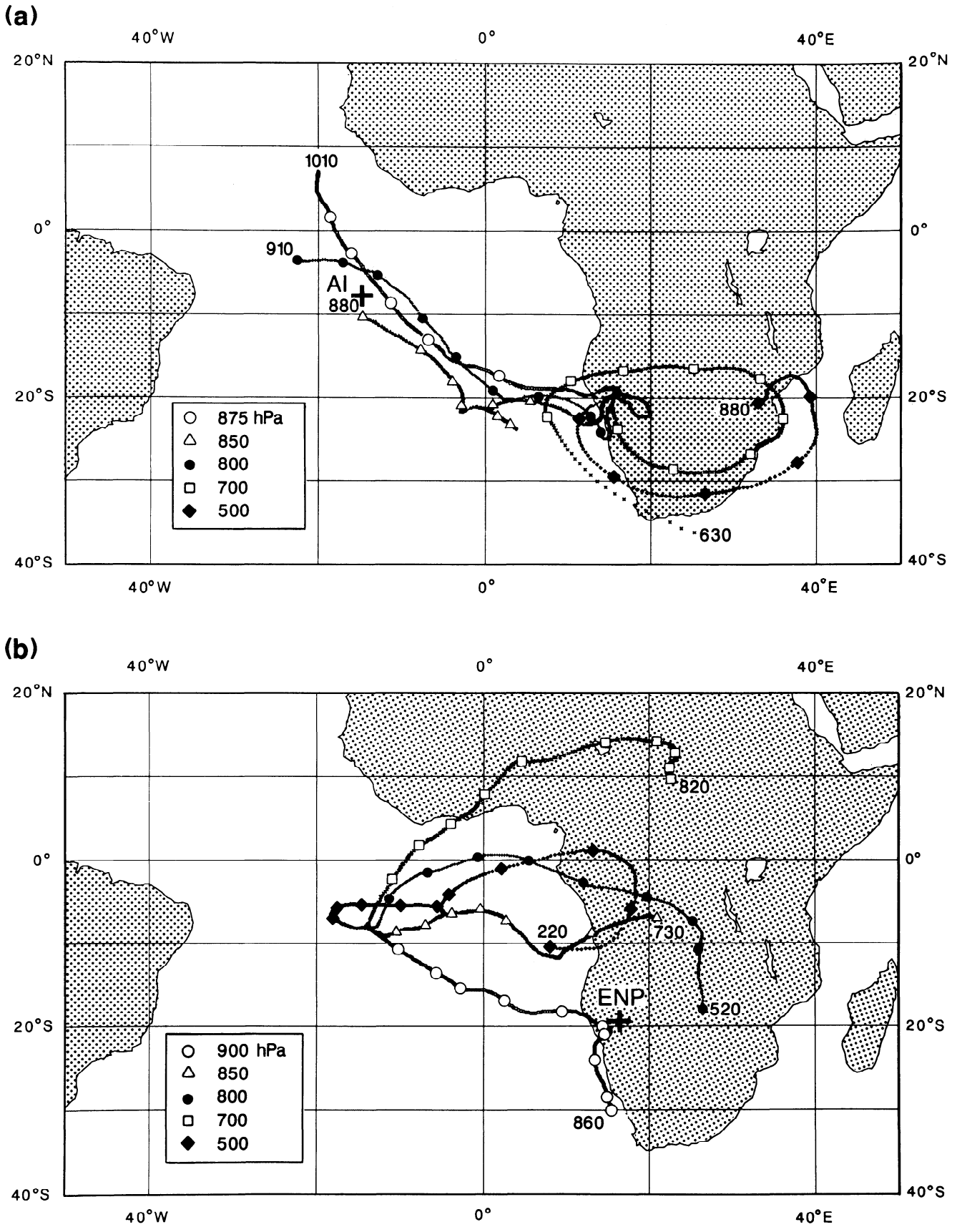

Figure 5. Forward and backward three-dimensional trajectories (a) from ENP on September 9, 1992, and (b) into AI on September 16, 1992. Five different initial trajectory levels are shown.

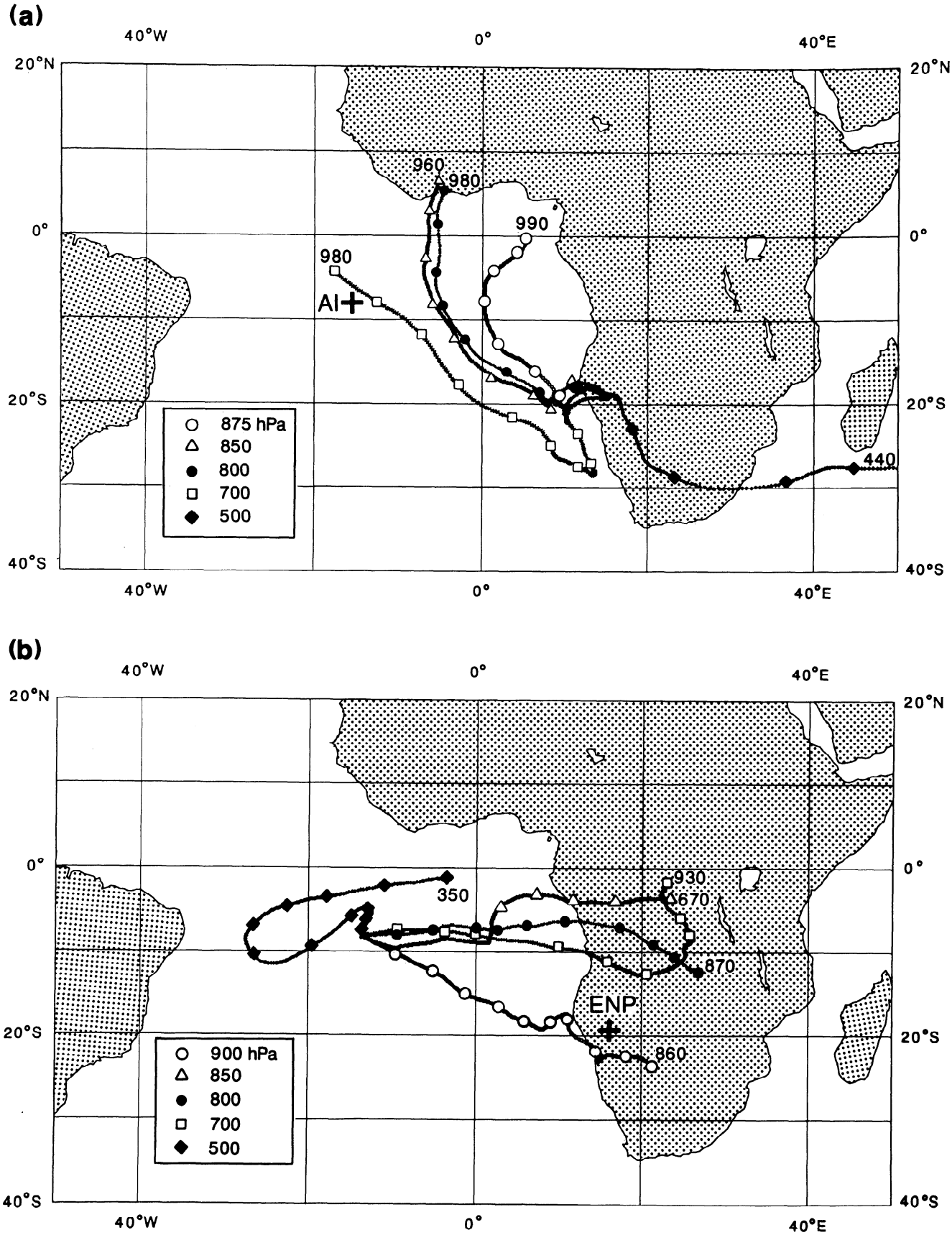

Figure 6. Forward and backward three-dimensional trajectories (a) from ENP on September 27, 1992, and (b) into AI on October 4, 1992. Five different initial trajectory levels are shown.

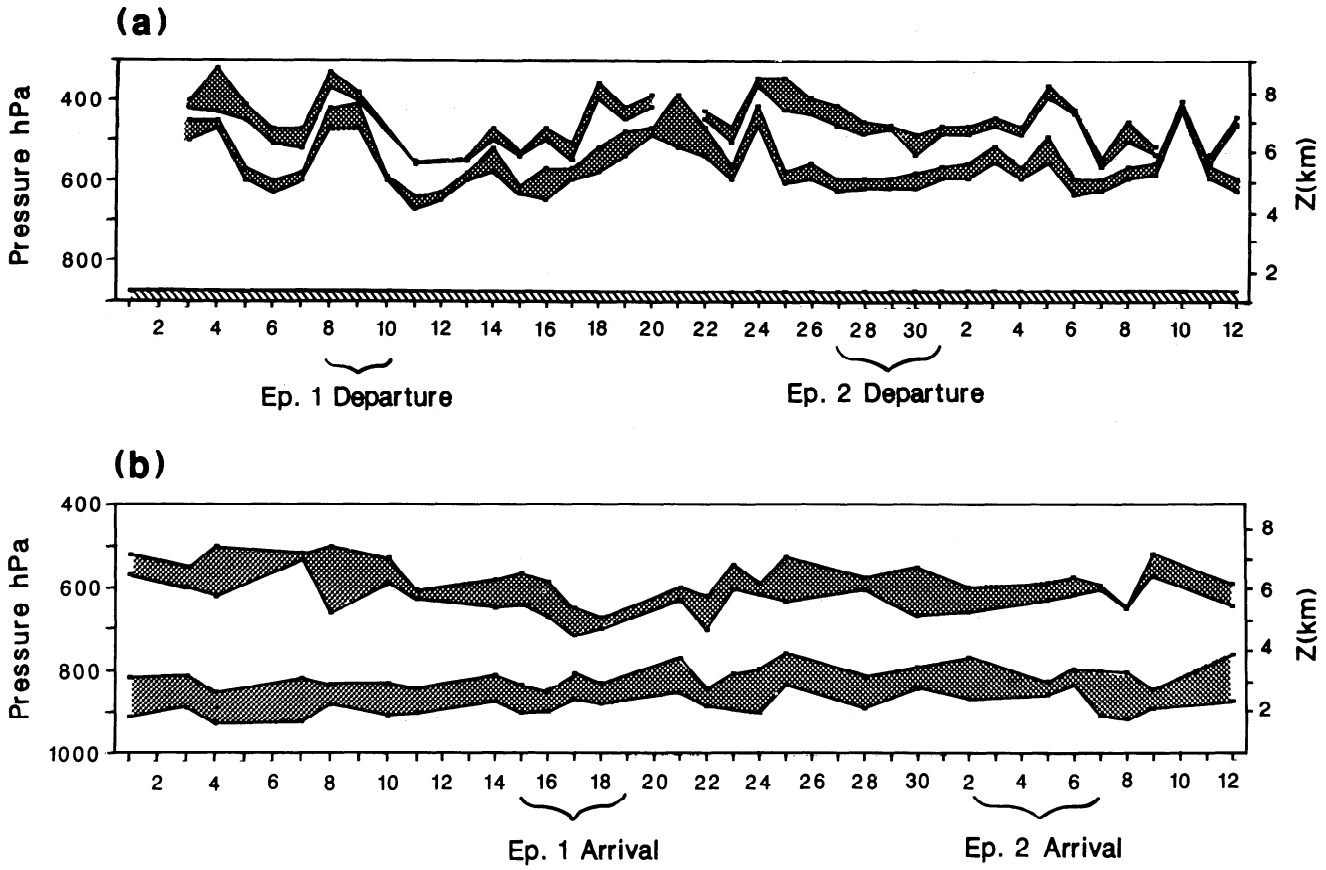

Figure 7. Layers of absolute stability for (a) ENP and (b) AI from September 1, 1992, to October 12, 1992. The levels are in meters above sea level and pressure (hectopascals).

Two layers of absolute stability are evident during the entire period over both the mid- Atlantic and northern Namibia. Over ENP the lower layer extends from 630 to 580 hPa and has a representative thickness of approximately 30 hPa (Figure 7a). The occasional disruptions of the lowest stable layer over ENP (September 8, 14, 20, and 24; October 5 and 10) are a result of the passage of travelling westerly wave disturbances.

The upper layer over ENP tends to be thinner and more variable fluctuating between the 500 and 400 hPa levels. The layers of absolute stability over AI are less variable, lower in height, and of greater vertical thickness than those over the subcontinent (Figure 7b). The lower-level base height of the trade wind inversion fluctuates between 900 and 830 hPa and has a representative thickness of about 65 hPa. The feature corresponds to the subsidence inversion observed over the continent [*Taljaard*, 1955; *Preston-Whyte et al.*, 1977] and the trade wind inversion over the Atlantic Ocean [*von Ficker*, 1936; *Riehl*, 1954]. The findings shown in Figure 7 correspond with height and agree in space with the more general results shown by *Garstang et al.* [this issue].

Air is transported offshore from Namibia en route to AI. The trajectory pathways of this transport are suppressed towards the surface by the subsidence occurring in the South Atlantic anticyclone (Figure 8). In all cases the trajectories failed to rise through the stable discontinuity of the trade wind inversion. Air originating over the plateau between the 875 and 800 hPa levels rises over the escarpment mountains before descending at a quasi-linear rate in its 6-to-7-day passage to the mid-Atlantic. At no time do the mountains of the escarpment or the escarpment itself (Figure 1) constitute any kind of impediment to westward flow, as has been suggested by *Krishnamurti et al.* [1993] and *Pickering et al.* [1994].

Subsidence rates may be determined both from the lowering of the base of the stable layer over the Atlantic Ocean and from the sinking trajectories. The vertical displacement of the latter is a direct product of the vertical velocities generated by the ECMWF model. Lowering of the stable layer suggests subsidence of about 225 m d^{-1} (Table 1). Sinking of trajectories suggest about 400 m d^{-1} (Table 1). These results are consistent with those of *Riehl* [1979] and *Newell et al.* [1972]. They differ considerably from those calculated by *Krishnamurti et al.* [1993].

Tables 2 and 3 trace the history of an air parcel arriving at AI to its source. Back trajectories are used in this analysis to determine the geographical location and height at which the transport was initiated 10 days earlier. Thereafter all trajectories are analyzed as if they were forward trajectories converging on AI. Thus back trajectories will be referred to as arriving at the island at different heights from different points of origin. Back trajectories starting at AI are calculated for each of 56 days (August 24 to October 18,1992). These back trajectories are divided into those arriving at AI in the lower (900, 850, and 800 hPa) and the middle troposphere (700 and 500 hPa). The 56 days and three levels yield a total of 168 trajectories arriving in the lower troposphere. The 56 days and two levels yield 112 trajectories arriving in the middle troposphere. The total number of back trajectories are traced back from AI through meridional planes on either side of the island. Each meridional

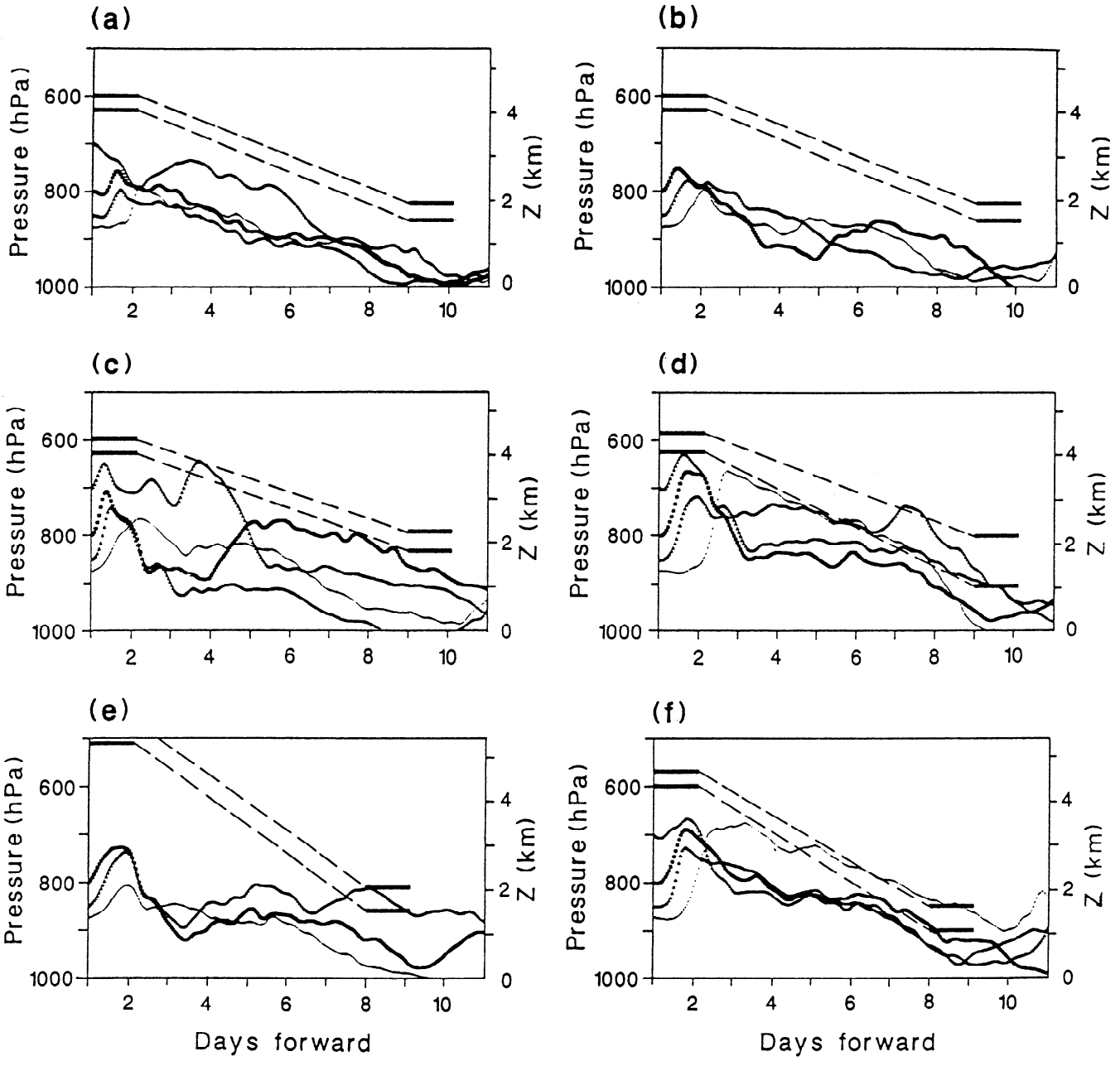

Figure 8. Vertical profiles of forward trajectories from ENP for (a) September 27; (b) September 28; (c) September 29; (d) September 30; (e) September 9; and (f) October 1, 1992. The trajectory heights are pressure (hectopascals) and height above sea level (meters). The dashed lines represent the inferred layer of absolute stability between ENP and AI.

plane extends from 10°N to 40°S latitude and from the surface to 300 hPa in the vertical. Table 2 shows the total frequency of back trajectories passing through each meridional plane and arriving in the lower and middle troposphere. The percentage of the total observed frequency relative to the total number of trajectories used is shown in parentheses. The total may exceed 100% when the trajectories pass through a meridional plane more than once (i.e., having recirculated).

Significant recirculation occurs in the central Atlantic at the prime meridian and at 10°W for air masses arriving at AI in the lower troposphere. Much less recirculation occurs with those arriving in the middle troposphere. This extensive recirculation at both levels provides more time for photochemic O_3 production and allows for new emissions to be added. The transport from the east (E) and from the west (W) is also shown in Table 2. Seventy-nine percent of the transport arriving in the lower troposphere at 10° and 15°W is from the east compared to 17% from the west. Of that arriving in the middle levels at AI, 69% is from the east and 26% from the west.

Table 3 shows the percentage of back trajectories from the east and from the west passing through each meridian for 10° latitudinal intervals between 10°N and 40°S. The percentages shown are calculated at each meridional plane (as opposed to a percentage of the total number of trajectories, as in Table 2).

Table 1. Vertical Motion (Subsidence) in the Lower Troposphere Between ~ 700 and 900 hPa Meters per Day and HectoPascals per Second Reported for the Tropical South Atlantic Ocean Between 20°S and 10°S Latitude

Source	Rate of Descent, m d^{-1}	Vertical Motion, hPa s^{-1}
Displacement of Stable Layers	200-250	$2.3\text{-}2.9 \times 10^{-4}$
Sinking of Trajectories	150-400	$1.7\text{-}4.6 \times 10^{-4}$
Riehl [1954, 1979]	100-600	$1.1\text{-}6.9 \times 10^{-4}$
Newell et al. [1972]	<100-500	0.5×10^{-4}
Krishnamurti et al. [1993]	1000-2000	$1.0\text{-}2.0 \times 10^{-3}$

Back trajectories for air arriving in the lower troposphere at AI at the longitude of 10°W, show that 79% of the transport originated from the east and 21% from the west. For air arriving in the middle troposphere at the same longitude, 84% of the backward trajectories are from the east and 16% from the west. The contributions from the east at each longitudinal wall increases eastwards reaching ~ 96% at 25°E in the lower troposphere for those back trajectories arriving at AI in the lower troposphere. In contrast, contributions from the east at each meridian fall off rapidly west of 15°W for those trajectories arriving in the lower troposphere. Only 8% of the back trajectories arriving at AI pass through 15°W from the east with the remaining 92% passing through 15°W from the west.

The most common pathway for lower-tropospheric air arriving from the east lies in a band from 0° to 10°S, where the frequency of back trajectories from AI does not fall below 42%. Significant transport from the east also occurs between 10° and 20°S and from 0° to 10°N. Trajectories from AI can be traced back into Africa at least to 30°E as far south as 20°S and north of 10°N. This region constitutes the main source region for acrosols and trace gases reaching the mid-Atlantic during SAFARI. Most importantly, it extends across a wide range of ecosystems and land surfaces, from deserts and arid savannas in the south through equatorial rain forests and into arid savannas to the north.

Back trajectories originating from the west reach maximum frequencies in the latitudinal band of 20° to 30°S for air that arrives at AI in the lower troposphere and in the band of 10° to 20°S for air in the midtroposphere. Backward trajectories from the west do not penetrate eastwards much beyond the Greenwich meridian. Trajectories which extend back toward the east tend to remain at their respective altitudes of origin in the lower and middle troposphere (Table 3). Trajectories extending backwards from AI to the west become elevated with time (and distance) from AI. These observations suggest a low-level origin in the east and an upper-level origin in the west for 10-day trajectories arriving at AI.

The most important synoptic scale feature influencing transports of aerosols over continental southern Africa is the anticyclonic circulation which dominates the mean flow pattern, reaching a maximum frequency of about 80% in midwinter

Table 2. Total Westerly and Easterly Trajectory Frequencies for Back Trajectories Arriving at Ascension Island in the Lower and Middle Troposphere

	Longitude, deg										
	30W	20W	15W	10W	0	10E	15E	20E	25E	30E	35E
Trajectories Arriving in the Lower Troposphere (900, 850, and 800 hPa)											
Frequency	23 (14)	29 (18)	38 (23)	224 (136)	223 (135)	101 (61)	91 (55)	77 (47)	52 (32)	35 (21)	16 (10)
West-East Frequency	22, 1 (13), (1)	28, 1 (17), (1)	35, 3 (20), (3)	47, 177 (28), (107)	53, 170 (32), (103)	5, 96 (3), (58)	6, 85 (4), (51)	6, 71 (4), (43)	2, 50 (2), (30)	3, 32 (2), (19)	1, 15 (1), (9)
Trajectories Arriving in the Middle Troposphere (700 and 500 hPa)											
Frequency	30 (27)	48 (44)	62 (56)	112 (102)	98 (89)	69 (63)	54 (49)	48 (44)	37 (34)	28 (25)	10 (9)
West-East Frequency	30, 0 (27), (0)	39, 9 (36), (8)	46, 16 (41), (15)	18, 94 (16), (85)	16, 82 (14), (75)	7 62 (6), (57)	3, 51 (3), (46)	6, 42 (5), (39)	4, 33 (4), (30)	6, 22 (5), (20)	1, 9 (1), (8)

Numbers in parentheses represent the percentage of counts relative to the total number of trajectories calculated for low level arrival of air (900, 850, and 800 hPa) out of 168 trajectories used and midlevel arrival of air (700 and 500 hPa) out of 112 trajectories used. Numbers exceeding 100% are indicative of multiple passes of trajectories through a particular meridional plane. Ascension Island is located at 14°W, 8°S.

Table 3. Percentages at Each Meridional Plane of Easterly and Westerly Frames of Ascension Island Back Trajectories During SAFARI (August 26-October 18, 1992) Arriving in the Lower and Middle Troposphere

Latitude, deg	Longitude, deg																					
	30W		20W		15W		10W		0		10E		15E		20E		25E		30E		35E	
Trajectories Arriving in the Lower Troposphere (900, 850, and 800 hPa)																						
10N	0	0	0	0	0	0	0	0	0	1	0	0	0	0	0	0	0	0	3	0	0	0
0-10N	0	0	0	0	0	0	1	5	0	11	1	24	1	26	1	23	0	15	0	11	0	0
10-0S	0	0	3	0	13	5	4	72* (850)	5	42* (800)	1	59* (700)	3	53* (700)	4	55* (650)	0	62* (700)	3	49* (600) (850)	0	69* (600) (900)
20-10S	26	4	31	3	26	3	5	1	11	22	3	12	1	12	3	14	4	19	6	28	6	25
30-20S	61* (550)	0	48* (550)	0	39* (550)	0	9	0	6	0	0	0	1	2	0	0	0	0	0	0	0	0
40-30S	9	0	14	0	13	0	2	1	2	0	0	0	0	0	0	0	0	0	0	0	0	0
TOTAL W-E	96	4	97	3	92	8	21	79	24	76	5	95	7	93	8	92	4	96	9	91	6	94
Trajectories Arriving in the Middle Troposphere (700 and 500 hPa)																						
10N	0	0	0	2	0	2	0	2	0	5	0	10	0	13	0	17	0	16	0	11	0	10
0-10N	0	0	0	10	0	16	0	27	0	46* (500)	1	52* (400)	0	55* (400)	2	42* (600)	0	30	0	18	0	20
10-0S	10	0	44* (500)	6	50* (500)	6	12	55* (700) (500)	11	33	3	28	2	26	2	25	3	38* (650)	14	46* (800)	0	60* (900)
20-10S	67* (400)	0	38	0	24	2	4	0	5	0	6	0	4	0	8	4	8	5	7	4	10	0
30-20S	23	0	0	0	0	0	0	0	0	0	0	0	0	0	0	0	0	0	0	0	0	0
40-30S	0	0	0	0	0	0	0	0	0	0	0	0	0	0	0	0	0	0	0	0	0	0
TOTAL W-E	100	0	82	18	74	26	16	84	16	84	10	90	6	94	12	88	11	89	21	79	10	90

Percentages are given for each latitudinal interval from 10°N to 40°S, and for each meridian (last row) for transport from the east (E) and from the west (W). The numbers in parentheses represent height in hPa of the locus of maximum transport. Cells with two heights indicated have flow equally split between low and midlevels. Ascension Island is located at 14°W, 8°S.
*Maximum westerly or easterly trajectory flow at that meridional plane.

[*Garstang et al.*, this issue]. Over the ocean to the west of southern Africa, the South Atlantic anticyclone likewise dominates the circulation. Only when easterly waves form over the heated arid western area of the subcontinent, mainly in summer, do conditions exist for the transport of aerosols and trace gases away from southern Africa (south of 20°S) and into the tropical South Atlantic Ocean. Such conditions only occurred on 4% of occasions during SAFARI.

4. Discussion and Conclusions

The analysis of stable isotopes of nitrogen and the multielemental analyses of surface aerosols collected at ENP and AI provide definite evidence that aerosol and air mass transport is taking place between these two specific sampling locations. The structural analysis of the atmospheric column shows pronounced and persistent stable layers occurring at the time of the measurements and extending over the space linking these points of observation. Trajectories which link the source (ENP) to the receptor (AI) and have simultaneous confirming chemical evidence are those at or below 800 hPa (~ 2000 m) and below the base of the observed stable layer. These trajectories, responding to ECMWF model-calculated vertical motion, subside at a rate generally consistent with the westward decrease in the height of the trade wind inversion.

Multielemental analysis of aerosol composition at the surface at ENP and AI suggests the sources of these aerosols. Non-sea-salt K and S indicate biomass burning and debris sources [*Losno et al.*, 1992; *Artaxo et al.*, 1993b], and Fe, Al, Si, and Ca are clear signals of terrestrial soil dust sources.

It is concluded that the nitrogen in the bulk stable isotopic signal comes from an enriched inorganic source associated with the soils of arid southwestern Africa. Such a source is consistent with the trajectory analysis. The enriched values may result from physical and microbial processes associated with desiccation, deflation and denitrification [*Schlesinger et al.*, 1990; *Williams et al.*, 1992]. G. Harris [personal communication, 1994] found highly elevated concentrations of biogenic nitrogenous emissions at low altitude (< 1 km) in the atmosphere in the ENP region during the period September 26-28, 1992. Nitrous oxide, N_2O, reached 3 ppbv, and NO, 0.8 ppbv at an altitude of ~ 80 m above the savanna. The profile of NO_x with height correlates with CO_2 but varies inversely with CO, suggesting a common biogenic source for NO_x and CO_2 and ruling out a fire related source (G. Harris, personal communication, 1994). J.S. Levine (personal communication, 1995) reported similar biogenic production of NO with the occurrence of early rains in the Kruger National Park in the southeastern region of the subcontinent. Active photochemical production of O_3 commences once NO levels exceed 10 pptv in an atmosphere containing abundant hydrocarbons and in the presence of high levels of solar insolation [*Crutzen*, 1973; *Chameides and Walker*, 1973; *Williams et al.*, 1992]. Further, these emissions could fractionate the stable isotopes of N allowing the residual N in the soils to become increasingly enriched. An enriched N signal may be associated with either soil dust, biogenic debris, microbial activity, or biomass burning particulates.

Results of the analysis of back trajectories for AI suggest that the major source region for air that reaches AI in the lower troposphere between 900 and 800 hPa lies over west Africa between 20°S and 10°N. This belt contains three distinctively different African biomes: equatorial rainforest, southern African woodland savanna, and northern African savannas.

At the time of the observations reported in this paper (September-October 1992), following an extreme drought in southern Africa, the primary source region of AI air masses (~ 55%) was concentrated between 0° and 10°S. The regions 0° to 10°N and 10° to 20°S contributed between 30 and 35% of the remaining transport from the east with slightly higher contributions coming from the latitudinal band between 0° and 10°N. Transport as seen from AI is limited to 30% or less from the west with the origin of the air elevated at the source to above 500 hPa. Transport from the east at AI in the latitudes south of 10°S is concentrated below 700 hPa. In the latitudinal band 0° to 10°S, the major corridor of low-level trajectory inflow, these transports are concentrated at or below 700 hPa.

Much of the air arriving in the midlevels at AI (between 700 and 500 hPa; 4-6 km) originates north of the equator (0° to 10°N) and above 600 hPa. The shift towards and subsequently north of the equator shifts the source-type region to the equatorial rain forests and to the savanna/Sahel boundary. Additionally, the rains have progressed at these latitudes well into the wet season (Figure 9) and biomass burning is at a minimum [*Cahoon et al.*, 1992]. Figure 9 shows the progression of the summer rains towards higher southern latitudes.

The latitudinal extent of the potential source regions for aerosols (and trace gases) reaching the central tropical Atlantic in the vicinity of AI therefore includes not only a broad range of ecosystems and surfaces but a range of connected processes which generate both aerosols and trace gases. The processes include production of aerosols from extremely dry surfaces (soils and vegetation), from rain forests, and from biomass burning. Processes producing trace gases of interest to the formation of tropospheric ozone include biogenic production of nitrogen species from the rain-wetted arid soils and hydrocarbons from the newly greening vegetation responding to the spring rains and biomass burning.

In regions influenced by the equatorial trough, some rain occurs in all months, and the dry season is shorter and much less defined (see Figure 9) than polewards from the trough. Biomass burning in the equatorial trough region is at a maximum during the short dry season. Since some level of moist convective mixing by cumuliform clouds is always present and the pronounced inversion layers discussed above are absent, vertical transport of surface-generated species in the trough region is possible. It is suspected that during SAFARI, between the latitudes of approximately 10°N and 10°S, biomass-burning products along with biogenic emissions were present at altitudes both below and above 700 hPa and were transported into the tropical South Atlantic in the middle and upper level flow. As products from the low-latitude region of Africa enter the south tropical Atlantic at altitudes above 700 hPa they will encounter a progressively stronger inversion below the level of transport. Penetration of that surface from upper levels will be inhibited and possibly even prevented.

A low tropospheric maximum in O_3 is observed in ozone soundings taken at ENP, AI, and Brazzaville during SAFARI. The height of this ozone maximum is as low as 500 m above the ground at ENP (~ 1.5-2 km) and as high as 4,000 m at AI (R.D. Diab, personal communication, 1995). The increase in lower tropospheric O_3 is consistent with the production of precursor gases from biogenic sources subject to the early spring rains and the generation of precursor gases due to biomass burning. Subsequent trapping of these gases by the low-level inversion, accumulations of precursor gases, as well as ozone below the inversion and subsequent transport into the tropical South Atlantic, would yield the observed increases in

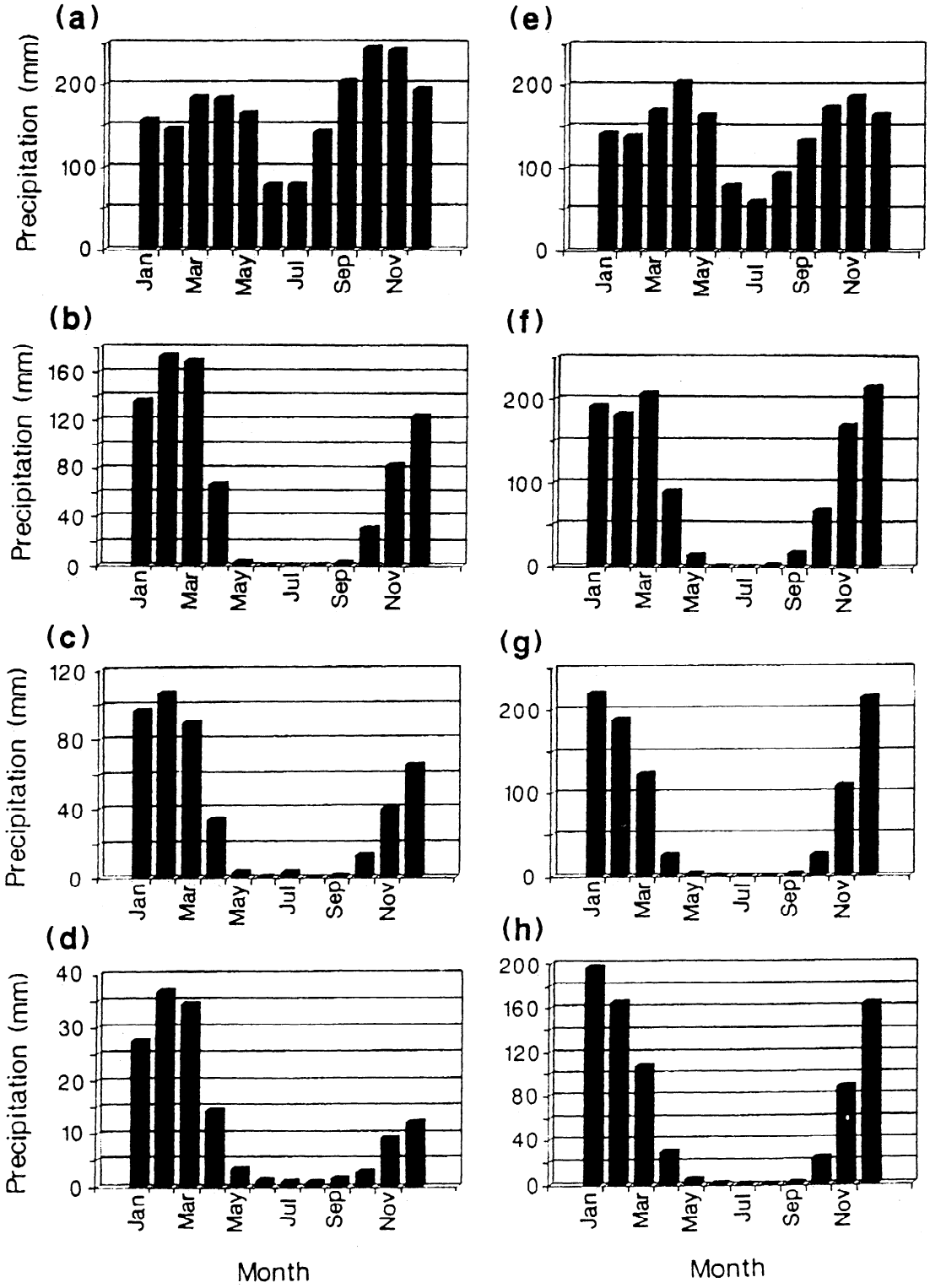

Figure 9. The progression of the southern African rainy season as illustrated by the mean monthly precipitation (millimeters per month) along two longitudinal transects (17°E, Figures 9a-9d; and 26°E, Figures 9e-9g) from the equator to approximately 20°S. The stations and their approximate locations are (a) Salonga, Zaire, 2°S, 21°E; (b) Bikuar/Mupa, Angola, 15°S, 15°E; (c) ENP, Namibia, 19°S, 16°E; (d) Namib/Nakluft, Namibia, 23°S, 15°E; (e) Maiko, Zaire, 2°S, 28°E; (f) Upemba, Zaire, 10°S, 27°E, (g) Kafue, Zambia, 15°S, 26°E; and (h) Chobe, Botswana, 18°S, 25°E. Rainfall data source: Global Change Database Project, 1990, sponsored by the International Council of Scientific Unions, International Geosphere-Biosphere Program and Panel for World Data Centers, Clark University, Worcester, Massachusetts.

O_3 both over the continent and over the tropical South Atlantic.

The existence at any particular time and location of a possible O_3 maximum, such as that identified by *Fishman et al.* [1991], will be a function of biogenic production, biomass burning, and the prevailing synoptic-to-planetary-scale circulation fields. Under extremely dry conditions it is hypothesized that any O_3 maximum will extend over the continent of southern Africa and into the Indian Ocean. During wet conditions it is believed that the synoptic-to-planetary-scale circulation fields will result in increased westward transport over the tropical South Atlantic leading to increased values of lower tropospheric O_3 over the tropical South Atlantic.

Acknowledgments. This work has been supported under grant ATM92-07924 from the National Science Foundation to the University of Virginia. Support of students in the field was also generously provided by the Eugene P. and William E. Odum Foundation. The South African Foundation for Research and Development provided support for both field and analytical work. Computational and graphics support were provided in part by VCR/LTER and NSF grants BSR8702333 and DEB-9211772. The trajectory calculations were carried out with the support of the Swedish Meteorological and Hydrological Institute and the European Centre for Medium-Range Weather Forecasts. This research is a contribution to the International Global Atmospheric Chemistry (IGAC) Core Project of the International Geosphere-Biosphere Programme (IGBP). We wish to thank all of the above organizations for their kind support. SAFARI was carried out with the approval and support of the governments of Namibia and South Africa. Field operations at the Etosha National Park were made possible by the Director and staff of the Etosha Ecological Institute and by the chief ranger and staff of Etosha National Park. Measurements at Ascension Island were made possible by the United States Air Force. We also wish to thank the Weather Services of Namibia and South Africa and our colleagues from the University of the Witwatersrand, University of Natal, University of Pretoria, and the South African Council for Industrial and Scientific Research for carrying out the observational program at Etosha National Park. W. Maenhaut is grateful to Irme Salma and Jan Cafmeyer for assistance. His research is supported by the Belgian State's Science Policy Office and by the Belgian "National Fonds voor Wetenschappelijk Onderzoek." P. Artaxo acknowledges financial support through grant 90/2950-2 from "FAPESP-Fundação de Amparo à Pesquisa do Estado de São Paulo."

References

Andreae, M. O., Soot carbon and excess fine potassium: Long-range transport of combustion derived aerosols, *Science, 220*, 1148-1151, 1983.

Andreae, M. O. et al., Biomass burning and associated haze layers over the Amazonian rain forest, *J. Geophys. Res., 93*, 1528-1550, 1988.

Andreae, M. O., J. Fishman, M. Garstang, J. G. Goldammer, C. O. Justice, J. S. Levine, R. J. Scholes, B. J. Stocks, A. M. Thompson, B. Van Wilgen, and the STARE/TRACE-A/SAFARI-92 Science Team, Biomass burning in the global environment: First results from the IGAC/BIBEX field campaign STARE/TRACE-A/SAFARI-92, in *Global Atmospheric-Biospheric Chemistry: The First IGAC Scientific Conference*, edited by R. Prinn, pp. 83-101 Plenum, New York,, 1993.

Annegarn, H. J., R. E. Van Grieken, D. M. Bibby, and F. Von Blottnitz, Background aerosol composition in the Namib Desert, South West Africa (Namibia), *Atmos. Environ., 17*, 2045-2053, 1983.

Artaxo, P., H. Storms, F. Bruynseels, R. Van Grieken, and W. Maenhaut, Composition and sources of aerosols from the Amazon basin, *J. Geophys. Res., 93*, 1605-1615, 1988.

Artaxo, P., W. Maenhaut, H. Storms, and R. Van Grieken, Aerosol characteristics and sources for the Amazon basin during the wet season, *J. Geophys. Res., 95*, 16,971-16,985, 1990.

Artaxo, P., F. Gerab, and M. L. C. Rabello, Elemental composition of aerosol particles from two background monitoring stations in the Amazon Basin, *Nucl. Instrum. Methods Phys. Res., Sect. B, 75*, 277-281, 1993a.

Artaxo, P., M. A. Yamasoe, J. V. Martins, S. Kocinas, S. Carvalho, and W. Maenhaut, Case study of atmospheric measurements in Brazil: Aerosol emissions from Amazon Basin fires, in *Fire in the Environment: The Ecological, Atmospheric and Climatic Importance of Vegetation Fires*, edited by P. J. Crutzen and J. G. Goldammer, pp. 139-158, John Wiley, New York, 1993b.

Bengtsson, L., Medium-range forecasting at ECMWF, *Adv. Geophys., 238*, 3-56, 1985.

Cachier, H., P. Buat-Menard, M. Fontugne, and J. Rancher, Source terms and source strengths of carbonaceous aerosol in the tropics, *J. Atmos. Chem., 3*, 469-489, 1985.

Cachier, H., P. Buat-Menard, M. Fontugne, and P. Chesselet, Long-range transport of continentally-derived particulate carbon in the marine atmosphere: Evidence from stable carbon isotope studies, *Tellus, 38*(B), 161-177, 1986.

Cahill, T. A., L. L. Asbaugh, J. B. Barone, R. Eldred, P. J. Feeney, R. G. Flocchini, C. Goodart, D. J. Shadoan, and G. Wolfe, Analysis of respirable fractions in atmospheric particles via sequential filtration, *J. Air Pollut. Control. Assoc., 27*, 675-678, 1977.

Cahoon, D. R., B. J. Stocks, J. S. Levine, W. R. Cofer, and K. P. O'Neill, Seasonal distribution of African savanna fires, *Nature, 359*, 812-815, 1992.

Chameides, W. L., and J. C. G. Walker, A photochemical theory of tropospheric ozone, *J. Geophys. Res., 78*, 8751-8760, 1973.

Chester, R., H. Elderfield, J. J. Griffin, L. R. Johnson, and R. C. Padgham, Eolian dust along the eastern margins of the Atlantic Ocean, *Mar. Geol., 13*, 91-105, 1972.

Connors, V. S., D. R. Cahoon, H. G. Reichle, E.-G. Brunke, M. Garstang, W. Seiler, and H. E. Scheel, Savanna burning and convective mixing in southern Africa: Implications for CO emissions and transport, in *Global Biomass Burning: Atmospheric, Climate and Biospheric Implications*, edited by J. S. Levine, pp. 147-154, MIT Press, Cambridge, Mass., 1991.

Crozat, G., Sur l'émision d'un aérosol riche en potassium par la forêt tropicale, *Tellus, 31*, 52-57, 1979.

Crozat, G., J. L. Domergue, J. Baudet, and V. Bogul, Influence des feux de brousse sur la composition chimique des aérosols atmosphériques en Afrique de l'ouest, *Atmos. Environ., 12*, 1917-1920, 1978.

Crutzen, P. J., A discussion of the chemistry of some minor constitutents in the stratosphere and troposphere, *Pure Appl. Phys., 106*, 1385-1399, 1973.

Fakhruzzaman, K. M., J. Fishman, V. G. Brackett, J. O. Kendall, and C. O. Justice, Large scale circulation patterns associated with high concentrations of tropospheric ozone in the tropical south Atlantic Ocean, *Proc. Quadr. Ozone Symp.*, NASA Conf. Publ. 3266, 158-161, 1994.

Fehsenfeld, F., et al., Emissions of volatile organic components from vegetation and the implications for atmospheric chemistry, *Global Biogeochem. Cycles, 6*, 389-430, 1992.

Fishman, J., Experiment probes elevated ozone levels over the tropical south Atlantic Ocean, *Eos Trans. AGU, 75*(33), 380, 1994.

Fishman, J., C. E. Watson, J. C. Larsen, and J. A. Logan, The distribution of tropospheric ozone determined from satellite data, *J. Geophys. Res., 95*, 3599-3617, 1990.

Fishman, J., K. Fakhruzzaman, B. Cros, and D. Nganga, Identification of widespread pollution in the southern hemisphere deduced from satellite analyses, *Science, 252*, 1693-1696, 1991.

Garstang, M., P. D. Tyson, R. Swap, M. Edwards, P. Kållberg, and J. A. Lindesay, Horizontal and vertical transport of air over southern Africa, *J. Geophys. Res.*,, this issue.

Hastenrath, S., *Climate Dynamics of the Tropics*, 488 pp., Kluwer Academic, Norwell, Mass., 1991.

Heaton, T. H. E., The 15N/14N ratios of plants in South Africa and Namibia: Relationship to climate and coastal/saline environments, *Oecologia, 74*, 236-246, 1987.

Heidam, N. Z., Review: Aerosol fractionation by sequential filtration with nuclepore filters, *Atmos. Environ., 15*, 891-904, 1981.

Johansson, S. A. E., and J. L. Campbell, *PIXE - A Novel Technique for Elemental Analysis*, 347 pp., John Wiley, New York, 1988.

John, W., S. Hering, G. Reischl, and G. Sasaki, Characteristics of nuclepore filters with large pore sizes, II, Filtration properties, *Atmos. Environ., 17*, 373-382, 1983.

Kållberg, P., Air parcel trajectories from analysed or forecast windfields, *Res. Dev. Notes 37*, Swed. Meteorol. and Hydrol. Inst. , Norrköping, 1984.

Krishnamurti, T. N., H. E. Fuelberg, M. C. Sinha, D. Oosterhof, E. L. Bensman, and V. B. Kuman, The meteorological environment of the tropospheric ozone maximum over the tropical south Atlantic Ocean, *J. Geophys. Res., 98*, 10,621-10,641, 1993.

Lacaux, J.-P., H. Cachier, and R. Delmas, Biomass burning in Africa: An overview of its impact on atmospheric chemistry, in *Fire in the Environment: The Ecological, Atmospheric, and Climatic Importance of Vegetation Fires*, edited by P. J. Crutzen and J. G. Goldammer, pp. 159-191, John Wiley, New York, 1993.

Lindesay, J. A., South African rainfall, the southern oscillation and a southern hemispheric semi-annual cycle, *Int. J. Clim., 8,* 17-30, 1988.

Losno, R., G. Bergametti, and P. Carlier, Origins of atmospheric particulate matter over the North Sea and the Atlantic Ocean, *J. Atmos. Chem., 15,* 333-352, 1992.

Macko, S. A., M. L. F. Estep, P. E. Hare, and T. C. Hoering, Isotopic fractionation of nitrogen and carbon in the synthesis of amino acids by microorganisms, *Isot. Geosci., 65,* 79-92, 1987.

Maenhaut, W., and H. Raemdonck, Accurate calibration of a Si (Li) detector for PIXE analysis, *Nucl. Instrum. and Methods Phys. Res., Sect. B, 1,* 123-136, 1984.

Maenhaut, W., A. Selen, P. Van Espen, R. Van Grieken, and J. W. Winchester, PIXE analysis of aerosol samples collected over the Atlantic Ocean from a sailboat, *Nucl. Instrum. and Methods Phys. Res., Sect. B, 181,* 399-405, 1981.

Maenhaut, W., I. Salma, J. Cafmeyer, H. J. Annegarn, and M. O. Andreae, Regional atmospheric aerosol composition and sources in the eastern Transvaal, South Africa, and impact of biomass burning, *J. Geophys. Res.,* this issue.

Newell, R. E., J. W. Kidson, D. G. Vincent, and G. J. Boer, *The General Circulation of the Tropical Atmosphere and Interactions with Extratropical Latitudes,* vol. 1, 258 pp., MIT Press, Cam bridge, Mass., 1972.

Parkin, D. W., D. R. Phillips, R. A. L. Sullivan, and L. R. Johnson, Airborne dust collections down the Atlantic, *Q. J. R. Meteorol. Soc., 98,* 798-808, 1972.

Pickering, K. E., A. M. Thompson, D. P. McNamara, and M. R. Schoeberl, An intercomparison of isentropic trajectories over the south Atlantic. *Mon. Weather. Rev., 122,* 864-879, 1994.

Preston-Whyte, R. A., and P. D. Tyson, *The Atmosphere and Weather of Southern Africa,* 374 pp., Oxford Univ. Press, New York, 1988.

Preston-Whyte, R. A., R. D. Diab, and P. D. Tyson, Towards an inversion climatology of southern Africa, II, Non-surface inver sions in the lower atmosphere, *S. Afr. Geogr. J., 59,* 47-59, 1977

Riehl, H., *Tropical Meteorology,* 392 pp., McGraw-Hill, New York, 1954.

Riehl, H., *Climate and Weather in the Tropics,* 611 pp., Academic San Diego, Calif., 1979.

Schlesinger, W. H., J. F. Reynolds, G. L. Cunningham, L. F. Huenneke, W. M. Jarrell, R. A. Virginia, and W. G. Whitford, Biological feedbacks in global desertification, *Science., 247,* 1043-1048, 1990.

Schutyser, P., W. Maenhaut, and R. Dams, Instrumental neutron activation analysis of dry atmospheric fall-out and rainwater, *Anal. Chim. Acta, 100,* 75-85, 1978.

Sealy, J. C., N. J. van der Merwe, J. A. Lee Thorp, and J. L. Lanham, Nitrogen isotopic ecology in southern Africa: Implications for environmental and dietary tracing, *Geochim.Cosmochim. Acta, 51,* 2707-2717, 1987b.

Siegfried, W. R., The incidence of veld-fire in the Etosha National Park, 1970-1979, *Madoqua, 12,* 225-230, 1981.

Swap, R. J., The transport characterization of southern African aerosols. Ph.D. dissertation, 170 pp., Univ. of Va., Charlottesville, 1995.

Taljaard, J. J., Stable stratification in the atmosphere over southern Africa, *Notos, 4,* 217-230, 1955.

Tapper, U. A. S., and K. G. Malmqvist, Analysis, imaging and modification of microscopic specimens with accelerator beams, *Anal. Chem., 63,* 715A-725A, 1991.

Tyson, P. D., *Climatic Change and Variability in Southern Africa,* 220 pp., Oxford Univ. Press, New York, 1986.

von Ficker, H., Die passatinversion, vol. 1, 33 pp., Veröffentlichungen Meteorol., Inst., Univ. Berlin, Berlin, 1936.

Williams, E. J., G. L. Hutchinson, and F. C. Fehsenfeld, NO_x and N_2O emissions from soil, *Global Biogeochem. Cycles, 6,* 351-388, 1992.

P. Artaxo, Institute of Physics, University of São Paulo, Caixa Postal 20516, CEP 01498-970, São Paulo, Brazil.

M. Garstang, S. A. Macko, R. Swap and P. D. Tyson, Department of Environmental Sciences, University of Virginia, Charlottesville, VA 22903.

P. Kållberg, European Centre for Medium-Range Weather Forecasts, Shinfield Park, Reading, Berkshire RG2 9AX, England.

W. Maenhaut, Institute for Nuclear Sciences, University of Gent, Proeftuinstraat 86, B-9000 Gent, Belgium.

R. Talbot, Institute for the Study of the Earth, Oceans and Space, University of New Hamsphire, Science and Engineering Research Building, Durham, NH 03824.

(Received July 20, 1994; revised March 4, 1995;
accepted March 10, 1995.)